A CONTRIBUTION TO ASSESSMENT OF STEAM GENERATOR TUBES INTEGRITY

Z. Tonković, I. Skozrit and J. Sorić
Faculty of Mechanical Engineering and Naval Architecture, University of Zagreb, 10000 Zagreb, Croatia

ABSTRACT

Three-dimensional linear and non-linear finite element analyses have been carried out to determine the stress intensity factors, the *J*-integral and the plastic limit loads for external axial semi-elliptical surface cracks in VVER steam generator tubes under internal pressure. Under the assumption of a small elastoplastic strain, the constitutive law characterizing the material's stress-strain response of the austenitic steel 08X18H10T is represented by the well-known Ramberg-Osgood model. All computations have been performed within the commercial finite element package ABAQUS. Six different crack lengths are considered (5, 10, 20, 30, 40 and 50 mm) and four values of the ratio of the crack depth to the tube thickness are selected (0.2, 0.4, 0.6 and 0.8). The results for the stress intensity factors and *J*-integral are generated and expressed as the GE/EPRI influence functions to allow comparisons with the values available in literature. As usual in literature, the plastic limit pressure solutions have been developed on the basis of finite element limit load analyses employing elastic-perfectly plastic material behaviour. Using these solutions, a new analytical approximation of the plastic limit pressure has been developed for a wide range of cracks. The proposed stress intensity factors, *J*-integral and the analytical approximation of limit pressure provide very useful tools for assessing the integrity of pressurized tubes. As an example, the Crack Driving Force (CDF) approach of the SINTAP procedure is applied to the failure analysis of steam generator tubes under internal pressure. The effects of crack depth and length on the failure pressure are evaluated for the tube geometry considered.

1 INTRODUCTION

Prediction of failure pressures of cracked steam generator tubes of the nuclear power plants has a critical issue on their safety. Operating experience with steam generators has shown that axial surface cracks present one of the most common causes of loss of steam generator tube integrity. An essential part of tube integrity analysis is how to estimate efficiently and accurately the plastic limit pressure and the fracture response characteristics, such as stress intensity factor (SIF) and *J*-integral of cracked tubes. In contrast to the internal axial semi-elliptical surface cracks [1], a very limited number of studies have been reported in the area dealing with the determination of the SIFs and *J*-integral for tubes with external axial semi-elliptical surface cracks [2]. Up to now, there have been no detailed 3-D finite element analyses (FEAs) for a wide range of surface cracks on the outside of a tube.

In some Failure Assessment Diagram methods, the limit load of a cracked tube is used to define a parameter L_r that measures the proximity to plastic collapse [3]. Furthermore, when a structural integrity assessment by using the R6 method [4] is performed, the reference stress is defined by the plastic limit load. Herein, the limit loads are usually estimated for defects in non-work-hardening materials [5, 6]. A great number of existing solutions for limit pressure of a cracked tube has been developed either analytically, based on a simple equilibrium stress field, or empirically, based on the test data [5]. These solutions are generally shown to be too conservative but the degree of conservatism can not be quantified. Recently, a finite element based plastic limit pressure expression for cylinders with external axial semi-elliptical surface cracks has been developed in reference [6]. However, the proposed expression is applicable to a very limited range of crack dimensions as shown in [7], and therefore the new extended solutions are desirable.

The goal of this paper is to obtain a new solution for the stress intensity factor, *J*-integral and the plastic limit pressure for VVER steam generator tubes with external axial surface cracks, which are subjected to internal pressure. To achieve this goal, both linear and non-linear 3D FE analyses based on deformation plasticity have been performed. These thick tubes are made of the austenitic steel 08X18H10T that corresponds to AISI 321 grade [8]. The FE solutions generated in this study have been used to develop the new influence coefficients of the stress intensity factor and *J*-integral as well as the analytical approximation of the plastic limit pressure for a wide range of external axial semi-elliptical surface cracks in tubes. The Crack Driving Force (CDF) approach of the European flaw assessment procedure SINTAP [3] is applied to the failure analysis of steam generator tubes under internal pressure. This study represents the continuation of our previous research presented in reference [7].

2 MATERIAL MODEL

The applied material model employs the J_2 deformation theory of plasticity and the small strain formulation. The stress-strain response of the austenitic steel 08X18H10T in the finite element analyses is described by the well-known Ramberg-Osgood model

$$\varepsilon / \varepsilon_0 = \sigma / \sigma_y + \alpha \left(\sigma / \sigma_y \right)^n , \qquad (1)$$

where σ_y is the yield stress, ε_0 is the associated reference strain $\varepsilon_0 = \sigma_y / E$ and E is the Young's modulus. The values α and n denote the parameters fitting the experimentally obtained curve. For the constitutive model presented, the material parameters, obtained experimentally [8], are summarised in Table 1. Herein, $J_{0.2}$ is the value of *J*-integral after 0.2 mm of blunting and ductile crack growth, which is good engineering approximation of fracture toughness.

Table 1: Mechanical properties of the austenitic steel 08X18H10T [8]

Temperature (^{0}C)	E (GPa)	σ_y (MPa)	σ_u (MPa)	α	n	$J_{0.2}$ (kJ/m^2)
20	209	250	560	1,920	4,59	210
300	184	160	420	1,375	4,01	160

3 FINITE ELEMENT ANALYSIS

Linear and non-linear finite element analysis has been performed to evaluate the stress intensity factor, *J*-integral and the plastic limit pressure for a tube with an external axial surface crack subjected to internal pressure p. Figure 1 shows the tube geometry and loading employed in the present work. The outer radius of the VVER tube R_0 is 8 mm and the wall thickness t is 1,5 mm (R_m/t=4.83). The crack is assumed to have a semi-elliptical shape described by a length $2c$, depth a and normalized crack length ρ, defined as $\rho = c / \sqrt{R_m t}$. Six different crack lengths were considered, $2c$ = 5, 10, 20, 30, 40 and 50 mm, and four values of the ratio of the crack depth to the tube thickness were selected, a/t = 0.2, 0.4, 0.6 and 0.8. As evident from Figure 1, the internal pressure p is described by the distributed load to the inner surface, together with an axial tension force P which is equivalent to the internal pressure acting on the closed end of the tube.

The finite element analysis is performed by using the commercial FE package ABAQUS/Standard [9]. A typical finite element mesh used in the analysis is shown in Figure 2. To avoid undesired finite element locking phenomena, 20-node brick elements (C3D20R) with reduced integration are used. Due to symmetry, only a quarter of the tube was modelled where the number of elements and nodes ranges from 2094 elements/10623 nodes to 8225 elements/39653 nodes. In order to model strain singularity at the crack tip correctly, the special collapsed wedge-shaped elements [9] are applied. The mesh refinement in the vicinity of the crack-tip is depicted in Figure 2b. The values of *J*-integral are computed around 5 contours surrounding the crack tip. The result from the 1st contour closest to the crack tip is discarded, and the value of J-integral is taken as the average of all values obtained from the 2nd to 5th contours.

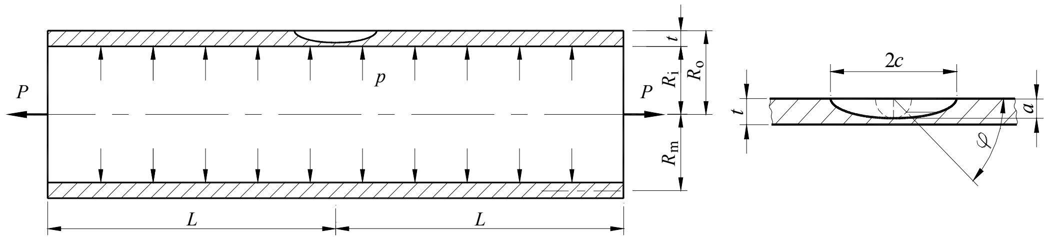

Figure 1: Geometry and dimensions of a tube subjected to internal pressure with an external axial semi-elliptical surface crack

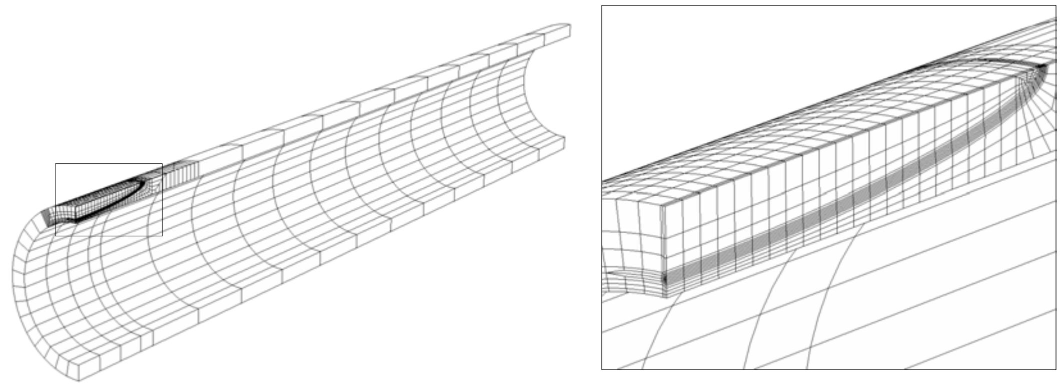

(a) (b)

Figure 2: Typical FE mesh for a tube with external axial surface crack ($2c$ = 20 mm, a/t = 0.8): (a) whole mesh; (b) crack tip mesh

3.1 Stress intensity factor

The linear-elastic FE computations yield the stress intensity factor K for an external axial surface crack in a tube under internal pressure, which may be expressed by the following relation [2]

$$K = \left(p\, R_m / t\right)\sqrt{\pi\, a}\, F\left(R_m / t, a/t, \rho, \varphi\right) , \tag{2}$$

where $F(R_m/t, a/t, \rho, \varphi)$ is a dimensionless function depending on the tube and crack geometry and φ is the angle defining the crack front position as shown in Figure 1. The values of the function $F(a/t, c)$ obtained by the FE analysis for the considered tube geometry are tabulated in Tables 2 and 3. As the SIF values reach their maximum at the deepest crack front location ($\varphi = \pi/2$), only the results at that critical location are given. In reference [7], a selected number of FEAs have been performed to validate the results of the stress intensity factor by comparing the computed values with the existing solutions.

Table 2: Dimensionless function F for the stress intensity factor ($2c$ = 5, 10 and 20 mm)

$2c$	5 mm				10 mm				20 mm			
a/t	0.2	0.4	0.6	0.8	0.2	0.4	0.6	0.8	0.2	0.4	0.6	0.8
F	0.992	1.125	1.204	1.184	1.039	1.331	1.680	1.967	1.060	1.451	2.045	2.797

Table 3: Dimensionless function F for the stress intensity factor ($2c$ = 30, 40 and 50 mm)

$2c$	30 mm				40 mm				50 mm			
a/t	0.25	0.4	0.6	0.8	0.2	0.4	0.6	0.8	0.2	0.4	0.6	0.8
F	1.150	1.492	2.173	3.129	-	1.516	2.240	3.279	-	1.530	2.282	3.376

3.2 Plastic limit pressure

In the elastic–perfectly plastic FE limit load analysis, the internal pressure was applied incrementally, until the collapse of the tube was indicated, by using the RIKS algorithm within ABAQUS [9]. This computational procedure gives the limit pressure p_L for a tube with an external axial surface crack. Based on the FE results, the empirical expression for the estimation of the plastic limit pressure in terms of non-dimensional crack configuration parameters a/t and ρ is derived, as follows:

$$p_L = (2/\sqrt{3})\sigma_Y \, ln\frac{R_o}{R_i}\left[A_0 + A_1(a/t) + A_2(a/t)^2\right] , \tag{3}$$

where
$$A_0 = 1, \quad A_1 = 0.14089 - 0.39607\rho + 0.06902\rho^2 - 0.00415\rho^3,$$
$$A_2 = -0.10307 + 0.00347\rho - 0.00969\rho^2 + 0.00094\rho^3. \tag{4}$$

For the considered ranges, this empirical relation predicts the limit pressure which differs less than 4% from values obtained by the FE computation. In the limit case of $a/t \rightarrow 0$, the above expression reduces to $p_L = 2/\sqrt{3}\,\sigma_Y \ln(R_0/R_i)$, which is the fully plastic collapse solution for an uncracked thick walled tube based on the Von Mises yield criterion. More detail about the proposed solution can be found in reference [7].

3.3 Elastoplastic J-integral

On applying the deformation theory of plasticity in the elastoplastic consideration, when the stress–strain curve is modeled by eqn (1), the total crack driving force J can be split into elastic and plastic parts, as

$$J = J_e + J_p . \tag{5}$$

Following reference [1], the plastic part of J-integral, J_p, for semi-elliptical surface cracked tubes can be given by

$$J_p = \alpha\sigma_y^2 / E(t-a)h_1(a/t, c)(p/p_L)^{n+1}, \tag{6}$$

where h_1 is the dimensionless plastic influence function which depends on the crack and tube geometry, while p_L is the plastic limit pressure from eqn (3). In order to obtain the values of the function $h_1(a/t, c)$, the plastic part of J integral is determined by

$$J_{p,FE} = J_{FE} - J_e \ , \tag{7}$$

and the values of function $h_1(a/t, c)$ are obtained by eqn (6). It is to note that the value of h_1 depends on the load magnitude, as shown in Figure 3. Since the power-law part of eqn (1) describing material behaviour during the loading process, is dominant at sufficiently large loads, the values of $h_1(a/t, c)$ at high loads should be taken from appropriate diagrams. The values of $h_1(a/t, c)$ for the considered tube geometry at the deepest crack front location ($\varphi = \pi/2$) are tabulated in Tables 4 and 5.

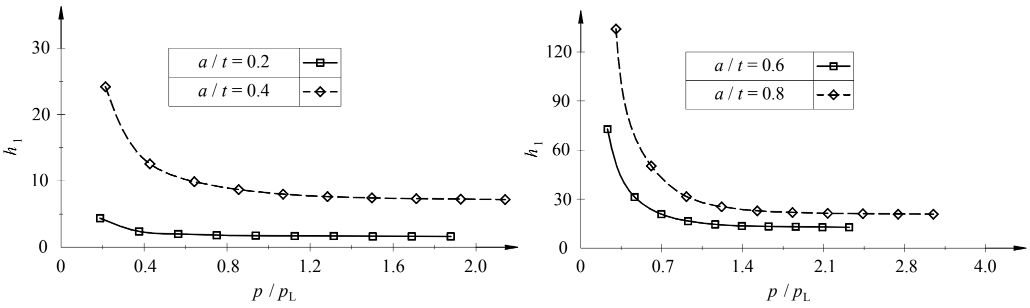

Figure 3: Variation of the plastic influence function h_1 with load magnitude for $2c$=20 mm

Table 4: Dimensionless function h_1 for the J-integral ($2c$ = 5, 10 and 20 mm)

$2c$	5 mm				10 mm				20 mm			
a / t	0.2	0.4	0.6	0.8	0.2	0.4	0.6	0.8	0.2	0.4	0.6	0.8
h_1	1.902	5.709	11.507	22.506	2.279	7.303	15.506	31.160	1.627	7.185	12.805	20.780

Table 5: Dimensionless function h_1 for the J-integral ($2c$ = 30, 40 and 50 mm)

$2c$	30 mm				40 mm				50 mm			
a / t	0.25	0.4	0.6	0.8	0.2	0.4	0.6	0.8	0.2	0.4	0.6	0.8
h_1	2.034	5.891	9.525	10.960	-	5.353	7.334	6.319	-	4.897	6.257	4.441

4 FAILURE ASSESSMENT ANALYSIS

The Crack Driving Force (CDF) approach of the SINTAP procedure [3] is applied to the failure analysis of steam generator tubes under internal pressure. Figure 4 shows the application of the CDF philosophies to the prediction of tube failure.

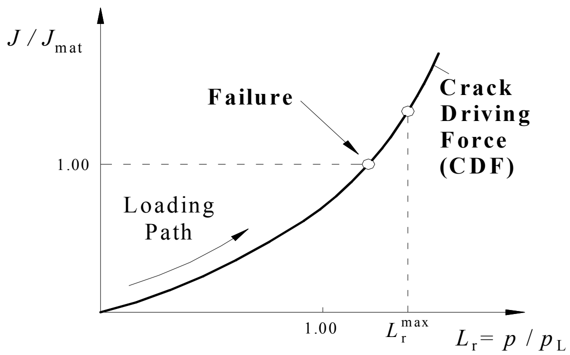

Figure 4: CDF analysis for prediction of failure

In the CDF approach J-integral is plotted and compared directly with the material's fracture toughness J_{mat}. Separate procedure is carried out for the plastic limit analysis. Herein, the plastic collapse limit is defined as

$$L_r^{max} = \sigma_f / \sigma_y , \tag{8}$$

where $\sigma_f = (\sigma_y + \sigma_u)/2$ is the flow stress [4]. Figure 5 shows the variations of the failure pressure with the crack length for different crack depths describing by crack depth to the tube thickness ratio, a/t = 0.2, 0.4, 0.6 and 0.8.

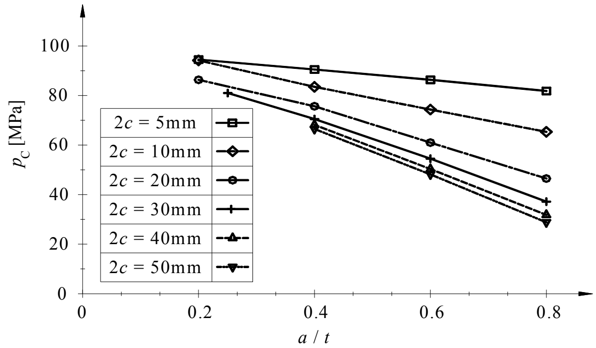

Figure 5: Failure pressure versus crack length for different depths

5 CONCLUSION

Using the detailed 3D linear and non-linear finite element analyses, the stress intensity factors, the *J*-integral and the plastic limit loads for the external axial semi-elliptical surface cracks in VVER steam generator tubes under internal pressure were computed. The results for the stress intensity factors and *J*-integral are presented in terms of the well-known GE/EPRI influence functions. The plastic limit pressure solutions were obtained by the finite element limit analyses using elastic-perfectly plastic material behaviour. These solutions were used to develop a new analytical approximation of the plastic limit pressure, which is applicable to a wide range of crack dimensions. Detailed results for the stress intensity factor and plastic limit pressure together with comparisons with available solutions are presented in reference [7]. In addition, the Crack Driving Force (CDF) approach of the SINTAP procedure was applied to the failure analysis of a steam generator tubes under internal pressure. The effects of crack depth and length on the failure pressure were evaluated.

REFERENCES

1. Kim, YJ., Kim, JS., Park, YJ. and Kim, YJ.: Elastic–plastic fracture mechanics method for finite internal axial surface cracks in cylinders, Engng Fract Mech, Vol. 71, pp. 925-944, 2004.
2. Raju, I.S. and Newman, J.C.: Stress-intensity factors for internal and external surface cracks in cylindrical vessels, J Pres Ves Tech, Vol. 104, pp. 293–298, 1982.
3 Zerbst, U., Hamann, R. and Wohlschlegel, A.: Application of the European flaw assessment procedure SINTAP to pipes, Int J Pres Ves Pip, Vol. 77, pp. 697-702, 2000.
4 Ainsworth, R.A.: The assessment of defects in structures of strain hardening material, Engng Fract Mech, Vol. 19, pp. 633–642, 1984.
5 Miller, A.G.: Review of limit loads of structures containing defects, Int J Pres Ves Pip, Vol. 32, pp. 191–327, 1988.
6 Kim, YJ., Shim, DJ., Nikbin, K., Kim, YJ., Hwang, SS. and Kim, JS.: Finite element based plastic limit loads for cylinders with part-through surface cracks under combined loading, Int J Pres Ves Pip, Vol. 80, pp. 527-540, 2003.
7 Tonković, Z. and Skozrit, I.: Elastoplastic analysis of external axial surface cracks in tubes, International Conference on Computational & Experimental Engineering and Sciences, Madeira, Portugal, 2004, accepted.
8 Timofeev, B.T., Karzov, G.P., Blumin, A.A. and Anikovsky, V.V.: Fracture toughness of austenitic welded joints, Int J Pres Ves Pip, Vol. 76, pp. 393-400, 1999.
9 ABAQUS User's guide and theoretical manual, Version 6.4, Hibbitt, Karlsson & Serensen, Inc., 2004.